CHEMISTRY OF MATERIALS

ARTICLE

pubs.acs.org/cm

Stöber Synthesis of Nitric Oxide-Releasing *S*-Nitrosothiol-Modified Silica Particles

Daniel A. Riccio, Julia L. Nugent, and Mark H. Schoenfisch*

Department of Chemistry, University of North Carolina at Chapel Hill, Chapel Hill, North Carolina 27599, United States

ABSTRACT: We report the synthesis of *S*-nitrosothiol-modified silica particles capable of nitric oxide (NO) release. The thiol precursor modification to form *S*-nitrosothiol NO donors was introduced into the silica network via co-condensation of mercaptosilane and alkoxysilane precursors. Both the concentration of reactants (i.e., water, ammonia, and silane) and the silane feed rate into the reaction proved important in the yield of monodisperse, spherical particles with tunable diameters ranging from 241−718 nm. Subsequent nitrosation resulted in NO storage approaching ~4.40 μmol NO mg^{-1}, as determined by total NO release. Behaving similar to low molecular weight *S*-nitrosothiol NO donors, the NO release from the macromolecular silica vehicles was influenced by light, temperature, and metal ions.

KEYWORDS: Stöber synthesis, silica particles, tunable size, nitric oxide release, therapeutic

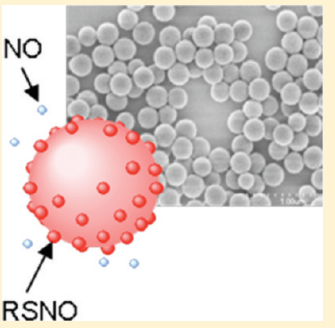

1. INTRODUCTION

Since the discovery of the physiological roles of nitric oxide (NO),[1−3] much research has focused on the synthesis of NO-releasing materials/vehicles to elicit NO's characteristics as an antimicrobial agent, mediator of wound repair, or angiogenic cofactor.[4−7] *S*-Nitrosothiols (RSNOs) are one class of endogenous NO donor believed to store/transport the majority of the body's natural reservoir of NO.[8−12] As such, a large body of work has utilized low molecular weight RSNOs (e.g., *S*-nitroso-glutathione (GSNO), *S*-nitroso-*N*-acetylcysteine (SNAC), and *S*-nitroso-*N*-acetyl-penicillamine (SNAP)) as donors to spontaneously release NO.[13−18] Although promising, the clinical application of low molecular weight NO donors has been slow because of both low NO storage (per donor molecule) and uncontrollable NO release kinetics. To address such shortcomings, we and others have conjugated NO donor precursors to larger scaffolds (e.g., proteins,[19−21] dendrimers,[22,23] and nanoparticles[24−28]), thus enabling high NO storage per delivery vehicle and release profiles similar to their small molecule analogues.

Silica particles are among the most widely employed macromolecular scaffolds for biomedical applications because of facile synthetic strategies and minimal cytotoxicity.[29] Previously, Frost and Meyerhoff grafted the surface of fumed silica particles (7−10 nm diameter) with SNAP, SNAC, and *S*-nitrosocysteine (CysNO) to create RSNO-modified silica particles.[30] However, the NO storage was limited to 0.021−0.138 μmol mg^{-1} because the thiol functionalization was restricted to the exterior of the particle. Alternatively, the hydrolysis and co-condensation of organosilane and tetraalkoxysilane precursors via sol−gel chemistry may represent a method for preparing a silica network with a larger concentration of organic functionalites.[31] Indeed, the Stöber process[32] (sol−gel chemistry with an alcohol solvent and an ammonia catalyst) has proven effective for synthesizing *N*-diazeniumdiolate-modified silica particles of diverse size and NO storage capacity.[24,25] The advantage of the Stöber method over surface grafting is that the co-condensation provides uniform incorporation of the organic (i.e., NO donor) functionality throughout the resulting silica network as opposed to restricted functionalization at the surface alone. As a result, such particles should exhibit significantly increased NO storage.

While reports have detailed the co-condensation of mercaptopropyltrimethoxysilane (MPTMS) and tetraethoxysilane (TEOS) to yield thiol-functionalized particles[33−41] and mesoporous materials,[42−44] NO storage/release was not their intended application. Although mesoporous materials offer a high degree of functionality, they consist of a vast, interconnected network and lack discrete particle morphology required for pharmacological therapies.[42−44] Mesoporous materials are thus more suited as adsorbents for environmental applications.[42−44] To date, co-condensation strategies for the synthesis of MPTMS-containing particles are complex and laborious,[34,35,37,40] often resulting in polydisperse aggregates[33,38,39,41] or a large size (1−100 μm).[34,36,37] Herein, we describe the Stöber synthesis of thiol-containing silica particles as a simple approach for creating spherical, monodisperse scaffolds for RSNO donors <1 μm in diameter. The effects of specific synthetic conditions (e.g., concentrations of water, ammonia, and silane and structure of silane precursors) on the resulting particle size and morphology are studied and optimized to yield monodisperse particles of tunable size, thiol functionality, and NO release.

2. EXPERIMENTAL SECTION

Materials. All solvents and chemicals were analytical-reagent grade and used as received unless noted otherwise. Tetramethoxysilane (TMOS) and *N*′,*N*-diisopropylethylamine were purchased from Sigma Aldrich (St. Louis, MO). 3-Mercaptopropyltrimethoxysilane (MPTMS), 3-mercaptopropylmethyldimethoxysilane (MPMDMS), and tetraethoxysilane (TEOS) were

Received: September 1, 2010
Revised: February 17, 2011
Published: March 07, 2011

purchased from Gelest (Tullytown, PA). Diethylenetriamine pentaacetic acid (DTPA) was purchased from Fluka (Buchs, Switzerland). 5,5′-Dithiobis-(2-nitrobenzoic acid) (DTNB, Ellman's reagent) was purchased from Invitrogen Molecular Probes (Eugene, OR). L-Cysteine-HCl-H_2O was purchased from Pierce-Thermo Fisher Scientific (Rockford, IL). Methyl sulfoxide was purchased from Acros (Morris Plains, NJ). Ethanol (EtOH), methanol (MeOH), and ammonia solution (NH_4OH, 30 wt % in water) were purchased from Fisher Scientific (Fair Lawn, NJ). Nitric oxide calibration gas (26.39 ppm; balance N_2) was purchased from National Welders Supply Co. (Durham, NC). Incandescent bulbs were purchased from Lowe's (Chapel Hill, NC). Distilled water was purified to 18.2 MΩ·cm with a Millipore Milli-Q Gradient A-10 water purification system (Bedford, MA).

Synthesis of Mercaptosilane-Based Silica Particles. Ratios of mercaptosilane and alkoxysilane (25−85 mol % MPTMS, balance TMOS or TEOS) (total silane volumes of 0.48−1.91 mL) were added either as a bolus injection or dropwise via a Kent Scientific Genie Plus syringe pump at a flow rate of 0.25−3.0 mL/min through an 18.5 gauge needle to a solution of ethanol (7.7−20.0 mL), water (0.0−17.7 mL), and ammonium hydroxide (1.0−12 mL). The total solution volume was 26.0 mL for all syntheses with a water concentration of 8.0 M. Upon increasing the water concentration to 16.1 M the ammonia and silane concentrations varied as follows. The total solution volumes were 26.7 and 28.8 mL when the silane concentration was 0.1 M and the ammonia concentrations were 3.3 and 5.5 M, respectively. The total solution volumes were 22.8, 26.2, and 31.1 mL when the silane concentration was 0.2 M and the ammonia concentrations were 1.9, 3.3, and 5.5 M, respectively. The total solution volume was 21.9, 24.9, and 27.4 mL when the silane concentration was 0.4 M and the ammonia concentrations were 1.9, 3.3, and 5.5 M, respectively. For syntheses with a water concentration exceeding 16.1 M, the total solution volume was 28.8 mL. Reactions were stirred for 2 h at room temperature, collected via centrifugation at 3645*g* (10 min), washed twice with 40 mL of EtOH, recollected, and dried overnight at ambient conditions.

Nitrosation of Mercaptosilane-Based Silica Particles. Thiols within the particles were nitrosated via reaction with nitrous acid.[12] Particles (∼200 mg) were first added to 4 mL of methanol (MeOH). While stirring, 2 mL of hydrochloric acid (5 M) was added to the suspension. Two mL of aqueous solution containing sodium nitrite (2× molar excess to thiol) and DTPA (500 μM) was then added to the particle suspension, and the mixture stirred for 2 h in the dark and on ice. Particles were collected by centrifugation at 3645*g* (5 min), washed with 40 mL of chilled 500 μM $DTPA_{(aq)}$, recollected, washed with 40 mL of chilled MeOH, recollected, and vacuum-dried for 30 min while shielded from light. Particles were stored at −20 °C in vacuo until further study.

Characterization of Mercaptosilane-Based Silica Particles. Solid-state cross-polarization/magic angle spinning (CP/MAS) ^{29}Si (71.548 MHz frequency) nuclear magnetic resonance (NMR) spectroscopy was performed on a Bruker 360 MHz DMX spectrometer (Billerica, MA). Particles were packed into 4 mm rotors and spun at 8.0 kHz. Spectra were collected at 5000 scans with the determination of chemical shifts in parts per million relative to an external TMS standard. Nitric oxide release was measured in real time (1 s intervals) using a Sievers NOA 280i Chemiluminescence Nitric Oxide Analyzer (NOA) (Boulder, CO). Calibration of the NOA was performed with both air passed through a Sievers NO zero filter and 26.39 ppm NO gas (balance N_2). Nitric oxide-releasing particles were immersed in 25 mL of deoxygenated solution and sparged with an 80 mL min^{-1} N_2 stream. Additional N_2 was supplied to the reaction flask to match the collection rate of the NOA at 200 mL min^{-1}. Temperature control was maintained using a water bath at 37 °C. Thermal and photoinitiated NO release were studied by conducting the experiments in 500 μM DTPA (pH 7.4 PBS) to chelate trace copper and illuminating the sample flask with 60, 100, and 200 W incandescent bulbs, respectively. Copper-initiated NO release was studied by adding the particles to 25 mL of 10 or 25 μM $CuBr_{2(aq)}$. The NOA sample flask was shielded from light with aluminum foil for experiments where light was not the intended initiator of NO release. Particle size was determined using a Zetasizer Nano ZS Particle Size and Zeta Potential Dynamic Light Scattering (DLS) Instrument (Malvern, U.K.). Samples were suspended in PBS at a concentration of 1 mg mL^{-1} and sonicated for 15 min prior to analysis. Scanning electron micrographs were recorded on a Hitachi S-4700 Scanning Electron Microscope (Pleasanton, CA). Nitrogen adsorption/desorption isotherms were obtained on a Micromeritics Tristar II 3020 Surface Area Analyzer (Norcross, GA). Samples were outgassed at 110 °C for 18 h with the specific surface area calculated using the Brunauer−Emmett−Teller (BET) method. Ellman's assay to test for free thiols was performed via adding known masses of particles to 2.5 mL of methyl sulfoxide and 1.5 mL of 10 mM Ellman's reagent stock in methyl sulfoxide. Solutions were diluted to a final volume of 6 mL with methanol, basified with 20 uL of diisopropylethylamine, and incubated for 1 h at room temperature. Thiol standards were prepared from a 15 mM cysteine stock solution in methyl sulfoxide and treated identically to the samples. Aliquots of 200 uL were pipetted into a 96-well microtiter plate, and the absorbance was recorded using a Labsystems Multiskan RC plate reader with an optical filter of 405 nm (Helsinki, Finland).

3. RESULTS AND DISCUSSION

3.1. Synthesis of Mercaptosilane-Based Silica Particles. Particle formation under the Stöber process proceeds upon hydrolysis and condensation of silane precursors where the relative hydrolysis rates for the precursors dictate both the speed of particle growth and the likelihood of each silane's incorporation into the silica network.[31,32,45,46] Excessive disparities between reaction rates of different silanes may lead to absence of particle formation upon attempted co-condensation. Our initial attempt to synthesize thiol-containing silica particles was based on a bolus injection of 3-mercaptopropyltrimethoxysilane (MPTMS) and alkoxysilane into an EtOH/NH_4OH solution. The resulting concentrations of ammonia, water and total silane were 3.3, 8.0, and 0.2 M, respectively. Tetramethoxysilane (TMOS) proved to be a sufficient backbone silane for co-condensation with MPTMS as their combination (at various mole percentages) resulted in the formation of a white precipitate (∼300 mg yield). Considering the slower hydrolysis rates of organosilanes compared to tetraalkoxysilanes, we expected that particles with greater mole percentages of TMOS would form more quickly than those with increasing amounts of MPTMS.[31,46] As indicated by visual onset of solution opacity, a marked increase in reaction time was observed upon increasing the concentration of MPTMS up to 85 mol %. At this concentration, the time to form a visible product after combining the silanes was roughly 15 min. Product formation at MPTMS concentrations >85 mol % was not observed. The inability to form particles at greater MPTMS concentrations may be attributed to the disparate hydrolysis rates between the silanes, suggesting that co-condensation requires a minimum concentration of the more readily hydrolyzable silane (i.e., TMOS) to initiate particle growth.[31,46] Materials synthesized via the co-condensation of MPTMS and tetraethoxysilane (TEOS) formed only in the concentration range of 75−85 mol % MPTMS. In contrast to the TMOS system, products with lower concentrations of MPTMS (e.g., 25 mol %) did not form using TEOS as a backbone, even at prolonged reaction times (up to 48 h). This result was not

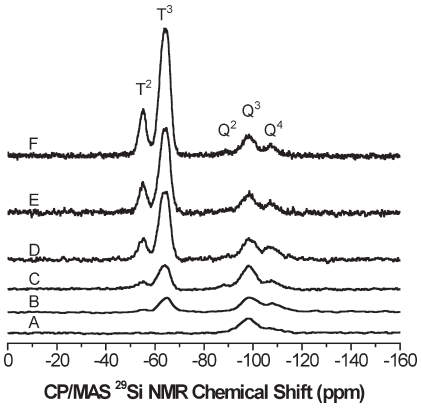

Figure 1. Solid-state cross-polarization/magic angle spinning (CP/MAS) ^{29}Si NMR spectra of silica synthesized with (A) 0, (B) 25, (C) 40, (D) 60, (E) 75, and (F) 85 mol % MPTMS (balance TMOS). Note: The Q and T bands have been designated.

unexpected based on the slower hydrolysis rate for TEOS compared to TMOS.[31,46]

We also evaluated the ability to form particles using 3-mercaptopropylmethyldimethoxysilane (MPMDMS) in our goal to understand the NO storage/release properties of another thiol-modified particle system. Unfortunately, the product yield (~5 mg) formed using MPMDMS with either TMOS or TEOS was significantly lower than MPTMS. The substitution of one of the hydrolyzable methoxy groups with a nonhydrolyzable methyl linkage in MPMDMS (vs MPTMS) likely decreases the resulting hydrolysis rate under basic conditions because of the inductive effect of electron density donation to the Si atom.[31,45,46] As a result, the reaction with hydroxide anion to hydrolyze the silane may be inhibited. Particle formation may be further diminished as each MPMDMS molecule is capable of forming only two siloxane bridges. Consequently, particle formation using MPMDMS was unsuccessful. Further studies were thus conducted using MPTMS-based particles.

To confirm the incorporation of mercaptosilane within the silica network and compare various compositions, solid-state ^{29}Si cross-polarization/magic angle spinning nuclear magnetic resonance (CP/MAS NMR) was used to characterize the MPTMS/TMOS products as a function of MPTMS concentration. Silicon atoms of tetraalkoxysilanes appear in the NMR spectra as Q^n bands while those of organotrialkoxysilanes appear as T^n bands. In both cases, n denotes the number of siloxane bonds attached to the Si atom.[47] The greater number of siloxane bonds to the Si atom, the further the NMR band shifts upfield. As shown in Figure 1, particles synthesized entirely from TMOS exhibited only Q bands. With increasing MPTMS concentration in the solution used to prepare the particles, the T bands increased relative to the Q bands, confirming greater incorporation of MPTMS in the silica particle.

Sulfur weight percent of each composition was determined using elemental analysis and further corroborated the covalent incorporation of the mercaptosilane. The weight percent of sulfur in the silica was 4.9, 7.1, 11.7, 13.6, and 17.3 for the 25, 40, 60, 75, and 85 mol % MPTMS (balance TMOS) compositions, respectively. The TEOS-based particles were found to have sulfur weight percents of 16.2 and 19.3 for 75 and 85 mol % MPTMS, respectively. As expected, the weight percent of sulfur increased linearly with increasing MPTMS concentration in the initial solution.

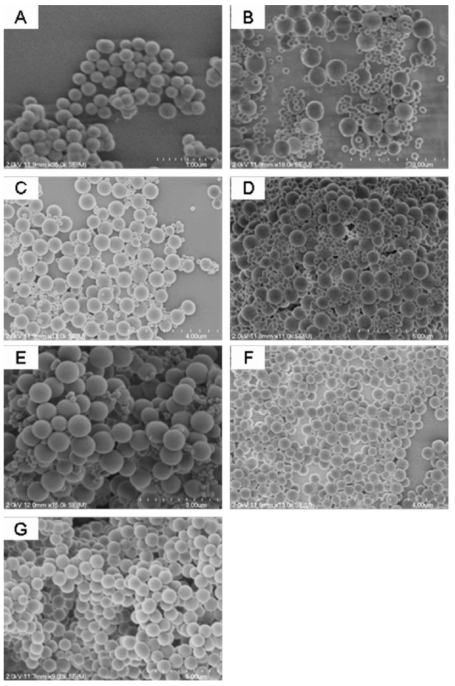

Figure 2. Scanning electron micrographs of (A) 25, (B) 40, (C) 60, (D) 75, and (E) 85 mol % MPTMS (balance TMOS) and (F) 75 and (G) 85 mol % MPTMS (balance TEOS) particles synthesized with 16.0 M water, 5.5 M ammonia, and 0.1 M silane.

Dynamic light scattering (DLS) measurements indicated that the sample was too polydisperse to accurately measure the particle size. Scanning electron micrographs (SEMs) further indicated that the thiol-containing silica was polydisperse and exhibited nonspherical morphology more indicative of colloidal silica than individual particles (data not shown).

We thus systematically varied synthetic parameters (i.e., water, ammonia, and silane concentrations) to tune the resulting particle morphology and achieve a more ideal spherical shape. The composition of 25 mol % MPTMS (balance TMOS) was chosen as the model system for comparison because of minimal organic character. Thus, the trends observed and previously reported for pure silica systems (i.e., TEOS)[32,48,49] could be applied to this system to guide the synthesis toward achieving spherical, monodisperse particles.

Ammonia Concentration and Water/Silane Ratio. The effects of reaction parameters and concentrations on particle morphology and size have been explored previously[32,48−54] For MPTMS particles, we found that increasing the water content from 8.0 to 16.2 M promoted the formation of spherical particles and prevented aggregation/fusion. This trend has been reported previously in the synthesis of TEOS particles where greater hydrolysis rates and larger, more spherical particles occurred with increasing water content.[50,53] Stöber et al. and Van Helden et al. also remarked that spherical particles were only observed in the presence of sufficient ammonia to promote complete hydrolysis of the silanes.[32,49] Lower ammonia concentrations were shown to result in particles that lacked spherical shape and aggregated.[52] Thus, we discovered that the ratio of water and ammonia to silane was a critical factor during particle synthesis. Upon considering all the data, we determined that the most ideal (spherical and monodisperse) 25 mol % MPTMS (balance TMOS) particles were formed using 5.5 M ammonia,

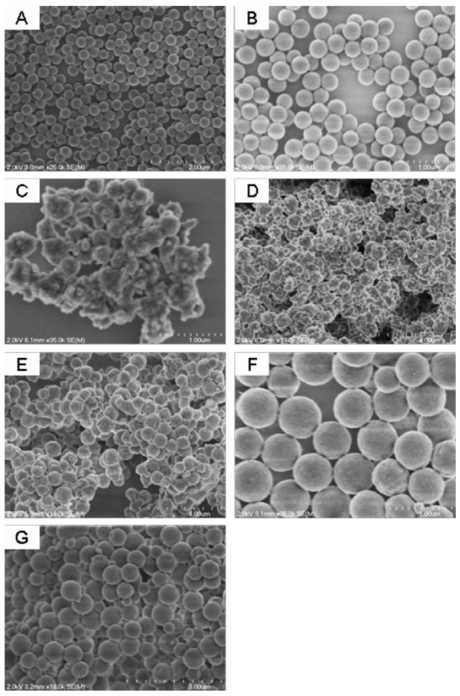

Figure 3. Scanning electron micrographs of (A) 25, (B) 40, (C) 60, (D) 75, and (E) 85 mol % MPTMS (balance TMOS) and (F) 75 and (G) 85 mol % MPTMS (balance TEOS) particles synthesized via a semibatch process with a silane feed rate of 0.5 mL min^{-1}.

0.1 M total silane, and 16.2 M water. Of note, the product yield (~70 mg) with this synthesis was lower than that obtained for the polydisperse colloidal silica. The decreased yield was expected because of the 4-fold decrease in the silane concentration used in the optimized synthesis.

Molar Percentage of MPTMS. Next, the concentration of MPTMS in the solution was increased to enhance the degree of thiol functionality and potential NO storage of the particles. Figure 2 depicts the resulting particles as the concentration of MPTMS was increased from 25−85 mol % and backbone alkoxysilane varied between TMOS and TEOS. As with the polydisperse colloidal silica system, the formation of particles was not observed for 25−60 mol % MPTMS (balance TEOS). Only 75 and 85 mol % MPTMS concentrations yielded particles with TEOS, illustrating how disparities in hydrolysis and condensation kinetics adversely affect and hinder particle formation. The 75 mol % MPTMS (balance TEOS) particles formed in a narrow size distribution and exhibited spherical morphologies (Figure 2F). In contrast, 85 mol % MPTMS (balance TEOS) particles appeared aggregated (Figure 2G). When using TMOS, 25 mol % MPTMS was the only concentration that yielded spherical, monodisperse particles (Figure 2A). Particles formed using ≥40 mol % MPTMS (balance TMOS) exhibited ideal morphologies, but with concomitant bimodal size distributions (Figure 2B-E).

Silane Feed Rate. Others have reported improvement in silica particle size monodispersity when using a syringe pump to flow one or more reactants (e.g., silane) into a vessel containing the other reactants at a constant rate.[53,55,56] Such a semibatch strategy decreases the instantaneous concentration of silane precursors allowing for a shorter particle nucleation period that narrows the size distribution of the resulting particles by

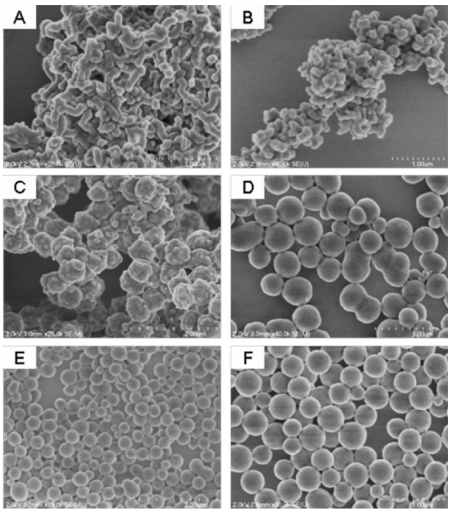

Figure 4. Scanning electron micrographs of 75 mol % MPTMS (balance TEOS) synthesized with (A) 47.0, (B) 42.0, (C) 40.6, (D) 36.5, (E) 32.5, and (F) 24.9 M water.

generating nuclei of similar sizes.[53] To remedy the bimodal size distribution that was observed for certain MPTMS compositions, we evaluated the effect of a silane feed rate of 0.5 mL min^{-1} on particle morphology throughout the range of compositions (Figure 3). As expected, the slower feed rate improved the dispersity of the already narrow size distribution for 25 mol % MPTMS (Figure 3A). A pronounced improvement in the monodispersity was also noted for 40 mol % MPTMS (balance TMOS, Figure 3B), with SEM indicating a particle diameter of 293 ± 24 nm. Slower silane feed rates (e.g., 0.25 mL min^{-1}) resulted in slight monodispersity improvements (data not shown), but at lower yields (e.g., ~40 vs 70 mg for 40 mol % MPTMS (balance TMOS) composition). Thus, 0.5 mL min^{-1} was determined to be the optimal feed rate as it allowed for a balance between sufficient particle yield and monodispersity. Similar to 25 mol % MPTMS (balance TMOS), the monodispersity of 75 mol % MPTMS (balance TEOS) improved, while the 85 mol % MPTMS (balance TEOS) system remained aggregated (Figure 3F and 3G, respectively). Additionally, the product yield increased to ~170 mg for these two compositions and can be attributed to the greater concentration of the larger MPTMS in the particles. Unfortunately, the semibatch process proved problematic for 60, 75, and 85 mol % MPTMS (balance TMOS) particles. As shown in Figure 3C−E, the slowed silane addition resulted in both aggregation and the formation of a large silica network rather than monodisperse, spherical particles. To examine this phenomenon further, silane feed rates were varied (0.25−3.0 mL min^{-1}) for 60 mol % MPTMS (balance TMOS). Feed rates <2.0 mL min^{-1} resulted in polydisperse, aggregated silica, while faster feed rates (2.0−3.0 mL min^{-1}) produced particles of a bimodal size (data not shown).

Water Concentration. While tailoring the size of their silica particles, Bogush et al.[48] and Stober et al.[32] both reported similar polydispersity and bimodal size distributions, exclusively for larger TEOS-based partcles. Thus, we attempted to decrease the size of the particles to improve particle monodispersity. The 75 mol % MPTMS (balance TEOS) particles were chosen as a model system to examine the effect of the water concentration on particle size and morphology. As shown in Figure 4, water

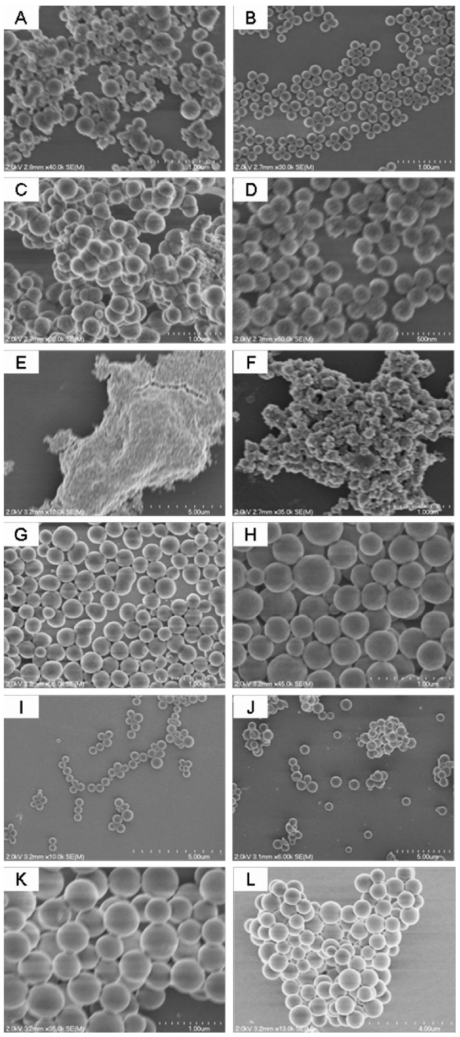

Figure 5. Scanning electron micrographs of (A-B) 25, (C-D) 40, (E-F) 60, (G-H) 75, and (I-J) 85 mol % MPTMS (balance TMOS) and (K-L) 85 mol % MPTMS (balance TEOS) particles synthesized with (A,C,E,F, G,I,K) 32.5 and (B, D, F, H, J, L) 24.9 M water.

concentrations ≥40.6 M favored rapid silane hydrolysis and condensation kinetics, leading to a highly condensed network rather than discrete, spherical particles. At a water concentration of 36.5 M, discrete particles were formed, but with morphologies featuring excessive aggregation. Monodisperse particles (333 ± 48 nm) were first observed at a slightly lower water concentration (32.5 M). As expected, particle size increased with decreasing water concentrations (456 ± 68 nm and 635 ± 63 nm for 24.9 and 16.2 M, respectively). Furthermore, the smaller particle sizes were accompanied with slightly lower yields for each composition. The yields for 75 mol % MPTMS (balance TEOS) particles were ∼65, 150, and 170 mg for water concentrations of 32.5, 24.9, and 16.2 M, respectively. The differences in yield may be factors of the efficiency of particle collection (i.e., centrifugation rpm and duration) for the smaller particles rather than chemical differences.

The optimal water concentrations (32.5 and 24.9 M) were next used to tune particle size and reduce the bimodal distribution characteristic of the 60, 75, and 85 mol % MPTMS (balance TMOS) particles. As shown in Figure 5, the intermediate water concentration (24.9 M) yielded particles with sizes of 179 ± 22 and 196 ± 25 nm for the 25 and 40 mol % MPTMS (balance TMOS) compositions, respectively. The greater water concentration (32.5 M) drastically increased the reaction kinetics for the mostly TMOS-based systems, resulting in highly fused silica networks. Increasing the concentration of MPTMS (75 mol %) yielded monodisperse, spherical particles of 363 ± 51 and 279 ± 49 nm using 24.9 and 32.5 M water, respectively. Aggregated and fused particles were formed for the greatest MPTMS concentration (85 mol %) when using 24.9 M water. However, monodisperse particles (440 ± 84 nm) were formed when synthesized with 32.5 M water. The TEOS-based counterpart to this system behaved similarly by yielding only discrete particles (506 ± 77 nm) when synthesized with the higher water concentration. At lower water amounts, the formation of aggregated particles was noted. The trend of decreasing particle yield with increasing water content that was observed for the 75 mol % MPTMS (balance TEOS) composition was mirrored for all other compositions evaluated. The yields for the 75 mol % (balance TMOS) particles decreased from ∼120 to 60 mg upon increasing the water content from 24.9 to 32.5 M. Likewise, the 25 mol % MPTMS (balance TMOS) particle yield decreased from ∼90 to 20 mg while the 40 mol % MPTMS system exhibited a decrease from ∼50 to 9 mg upon increasing the water concentration from 16.2 to 24.9 M. The yields for both 85 mol % MPTMS compositions (i.e, TMOS and TEOS balance) at a water concentration of 32.5 M were ∼160 mg.

Perhaps of greatest significance, the elevated water concentrations used to synthesize the thiol-modified particles successfully resolved the bimodal nature of certain compositions not resolvable using a semibatch process alone. Of note, 60 mol % MPTMS (balance TMOS) was the only composition that consistently yielded particles of a bimodal nature. Increasing the water content regardless of addition method (bolus vs semibatch) always resulted in a highly fused silica network. Branda et al. have shown that when alkoxides are mixed during co-condensation, the size distribution of formed nuclei is widest when the ratio of the alkoxides is closest to 0.5 as is the case for this composition that contains a mixture of organosilane and alkoxysilane in almost equal amounts.[57]

Particle sizes were also measured by DLS to corroborate particle monodispersity and size measured using SEM. The combination of DLS and SEM analysis was crucial for obtaining an accurate characterization of particle size. Although not often used together for characterizing silica particles, their combination was necessary to affirm spherical particle morphology for DLS size determination. As shown in Table 1, the DLS measurements were in agreement with the sizes calculated from the SEM images. The slightly increased average diameters observed with DLS may be attributed to the solvent sphere that increases the hydrodynamic radius or via direct hydration of the silica particles themselves (DLS measurements conducted in solution). Like SEM, the DLS measurements indicated a narrow size distribution, as evidenced by low polydispersity indices for each composition. For monodisperse silica particles, the PDI was <0.070 while aggregated silica (e.g., 85 mol % MPTMS particles synthesized with 24.9 M water) were characterized as having a PDI of 0.16−0.20. Of note, PBS was used as a dispersant for compositions with large MPTMS concentrations. However, smaller particles with a large degree of inorganic character (i.e., ≤40 mol % MPTMS) aggregated in this dispersant resulting in erratic DLS measurements (i.e., increasing photon count rate indicative of sample aggregation). This aggregation may be

Table 1. Particle Diameters of S-Nitrosothiol-Modified Silica Particles

particle composition (mol % MPTMS)	water content (M)	particle size[a] (nm)	Z-average size[b] (nm)	polydispersity index
75 (balance TEOS)	32.5	333 ± 48	416.2 ± 23.4	0.027
75 (balance TEOS)	24.9	456 ± 68	529.6 ± 23.7	0.018
75 (balance TEOS)	16.2	635 ± 63	718.0 ± 51.7	0.046
85 (balance TEOS)	32.5	506 ± 77	668.7 ± 46.0	0.040
25 (balance TMOS)	24.9	179 ± 22	258.4 ± 15.1[c]	0.031
25 (balance TMOS)	16.2	252 ± 20	469.0 ± 24.8[c]	0.025
40 (balance TMOS)	24.9	196 ± 25	240.7 ± 17.9[c]	0.064
40 (balance TMOS)	16.2	293 ± 24	404.8 ± 28.2	0.045
75 (balance TMOS)	32.5	279 ± 49	431.2 ± 29.5	0.043
75 (balance TMOS)	24.9	363 ± 51	507.6 ± 30.8	0.032
85 (balance TMOS)	32.5	440 ± 84	696.2 ± 44.4	0.042

[a] Size calculated from scanning electron micrographs of $n = 120$ particles. [b] Sizes acquired from dynamic light scattering measurements in pH 7.4 PBS for $n = 3$ syntheses. [c] Ethanol used as dispersant.

Table 2. Elemental Analysis, Nitric Oxide Storage, and Porosity of S-Nitrosothiol-Modified Silica Particles

particle composition (mol % MPTMS)	water content (M)	sulfur content[a] (wt %)	total NO released[c] (μmol mg^{-1})	nitrosation efficiency (%)	specific surface area[d] (m^2 g^{-1})
75 (balance TEOS)	32.5	13.8 ± 3.0	3.24 ± 0.61	75.1 ± 21.6	8.99 ± 0.24
75 (balance TEOS)	24.9	16.0 ± 1.7	3.58 ± 0.39	71.7 ± 10.9	7.69 ± 0.16
75 (balance TEOS)	16.2	15.6 ± 1.9	3.15 ± 0.60	64.7 ± 14.6	3.87 ± 0.13
85 (balance TEOS)	32.5	20.0 ± 3.9	3.95 ± 0.66	63.3 ± 16.2	4.16 ± 0.19
25 (balance TMOS)	24.9	<0.0[b]	0.09 ± 0.02	NA	54.90 ± 1.53
25 (balance TMOS)	16.2	0.5 ± 0.4	0.10 ± 0.02	62.9 ± 45.7	60.11 ± 1.93
40 (balance TMOS)	24.9	1.1 ± 0.6	0.34 ± 0.02	100.3 ± 53.8	51.85 ± 0.74
40 (balance TMOS)	16.2	3.1 ± 2.6	0.52 ± 0.22	54.2 ± 50.7	91.39 ± 4.03
75 (balance TMOS)	32.5	18.3 ± 5.3	3.31 ± 0.85	58.0 ± 22.6	10.76 ± 0.30
75 (balance TMOS)	24.9	15.3 ± 5.3	3.73 ± 0.62	78.2 ± 30.1	6.77 ± 0.13
85 (balance TMOS)	32.5	20.6 ± 5.7	4.39 ± 0.02	68.5 ± 19.0	4.09 ± 0.25

[a] Average weight percents are calculated from $n = 3$ syntheses. [b] Weight percent was less than instrument limit of detection. [c] Averages are calculated from $n = 3$ syntheses and after 5 h of 200 W irradiation. [d] Calculated from nitrogen adsoprtion and Brunauer−Emmett−Teller analysis of $n = 3$ measurements.

attributed to a large surface density of protonated silanol groups leading to unfavorable particle interaction. While basic conditions resulted in inconsistent DLS measurements because of particle dissolution, ethanol was a viable alternative dispersant as evidenced by the correlation between DLS and SEM measurements.

Elemental analysis was used to characterize the composition of the particles. As expected, the weight percentages of sulfur in the particles increased accordingly with the MPTMS mol % used to make the particles indicating incorporation of the thiol functionality (Table 2). Syntheses promoting the formation of discrete, spherical particles tended to be preferentially derived from one precursor as evidenced by a large gap in the transition from 40 to 75 mol % MPTMS (3.08 ± 2.57 and 15.62 ± 1.90 wt %, respectively). These values were in marked contrast to the sulfur wt % of the colloidal silica. Although the increased sulfur wt % values were more linearly proportional for the colloidal silica, the lack of discrete, spherical particles was not ideal. The comparison of the two syntheses and systems (colloidal vs discrete particles) reveals that a delicate balance exists between silane incorporation and certain design criteria (i.e., spherical particle formation).

3.2. Nitrosation of Mercaptosilane-Based Silica Particles. The MPTMS-modified particles were nitrosated to enable NO storage and release. Briefly, the particles were treated with acidified sodium nitrite, generating nitrous acid, a nitrosating agent that reacts with thiols to form RSNOs (eq 1).[12]

$$RSH + HNO_2 \rightleftarrows RSNO + H_2O \quad (1)$$

Since RSNOs prepared from primary thiols absorb light at 330−350 and 550−600 nm,[12,58,59] successful RSNO formation was confirmed by the resulting red color of the particles after nitrosation. Furthermore, the intensity of the color increased with MPTMS mol % indicating greater RSNO formation.

Scheme 1. RSNO Decomposition Pathways

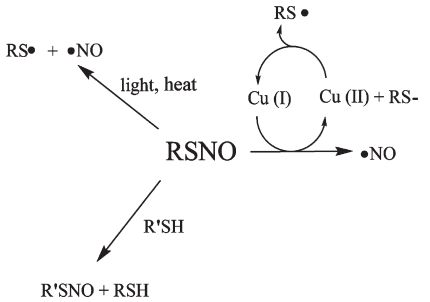

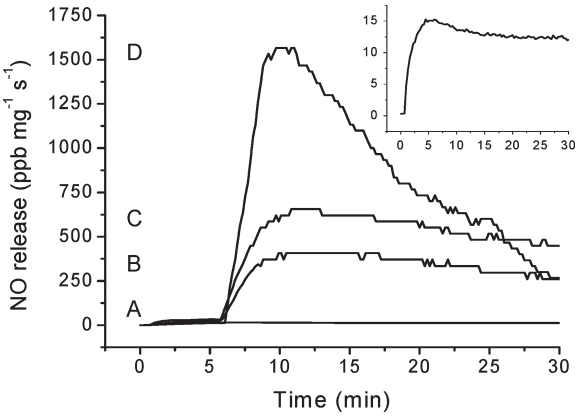

Figure 6. Representative nitric oxide release from RSNO-modified 75 mol % MPTMS (balance TEOS) particles in the presence of (A) 0, (B) 60, (C) 100, and (D) 200 W irradiation at 0 °C. [Inset: Enlarged view of A.].

As shown in Scheme 1, *S*-nitrosothiols decompose via a multitude of pathways.[12,58] Both photo and thermal irradiation of RSNOs result in homolytic cleavage of the S−N bond, yielding NO and a thiyl radical. The thiyl radical may subsequently react with an RSNO to generate a disulfide and an additional equivalent of NO.[12,58] Dicks et al. have shown that Cu(I), resulting from the reduction of Cu(II) via trace thiolate ions, is active in a catalytic RSNO decomposition mechanism.[60] Transnitrosation between a thiol and an RSNO may also occur, resulting in the transfer of the nitroso functionality and formation of a new RSNO species that may decompose via the aforementioned pathways.[12,58]

To assess the NO storage and release, RSNO-modified particles (∼2 mg) were added to 500 μM DTPA (pH 7.4 PBS) at a temperature of 0 °C, while measuring the ensuing NO release as a function of photolytic decomposition. As shown in the representative NO release profiles in Figure 6, RSNO-modified silica particles exhibited photoinitiated release of NO upon exposure to broadband, white light. Greater irradiation levels (i.e., power) resulted in elevated NO release from the particles. Of note, low levels of NO release (∼15 ppb mg^{-1} s^{-1}) were observed at 0 °C and in the dark (Figure 6 inset) illustrating an inherent thermal instability of these particles, as is common with primary-derived RSNOs.[58] Others have shown that oxygen may react with NO to form dinitrogen trioxide (N_2O_3), an oxidant that also decomposes RSNOs.[61] These issues evoke concern regarding the stability of these particles and their eventual utility for certain biomedical applications. Both the elimination of oxygen from the storage environment of the RSNO-modified particles and lower temperatures would be expected to increase the NO storage stability of the particles. Indeed, the NO release capacity after 2 months of storage at −20 °C in vacuo and in the dark was identical to freshly nitrosated particles illustrating that proper storage conditions extend particle stability and maintain their potential pharmacological utility. Furthermore, doping RSNO donors within a polymeric matrix has been shown to enhance their thermal stability because of a cage effect resulting in recombination of thiyl and NO radicals after homolysis.[62] We hypothesize that RSNO particle-doped polymers would further enhance the stability of these NO release vehicles. Such work is the subject of current research in our laboratory in an effort to create antibacterial polymers with extended NO release ability.

Because of the rapid kinetics of the photoinitiated decomposition, total NO storage of the particles was assessed by exposing the particles to 200 W of broadband light. Indeed, >95% of the NO stored was released after 5 h of irradiation at 200 W. As given in Table 2, the total NO released from the particles ranged from 0.09−4.39 μmol mg^{-1}. These levels of NO storage are an order of magnitude larger than previously reported RSNO-modified silica particles.[30] Using the average sulfur weight percents in conjunction with the average NO storage values, the percent conversion of thiol to RSNO for each particle composition was calculated (Table 2). Although large, the nitrosation efficiency does not reach 100% for the majority of compositions. Thiols that exist as disulfides or that are inaccessible to the nitrosating agent likely are responsible for incomplete nitrosation. To investigate these hypotheses, the Ellman's assay was used to quantify the amount of reduced thiols for comparison to the total sulfur content of the particles as discerned from CHN/S elemental analysis. For the 25 and 40 mol % compositions, the elemental analysis results were comparable to the free thiol content deduced by the Ellman's assay (data not shown). However, the free thiol values for compositions above these MPTMS concentrations were superficially low when viewed in relation to the total NO storage. We hypothesize that this discrepancy is due to the thiols being accessible to nitrous acid, but not to the bulkier (i.e., larger) Ellman's reagent. The molecular size of Ellman's reagent has been cited previously to be problematic in quantifying thiols embedded within bulk materials.[63] Furthermore, the assay requires significant method development when attempting to analyze thiols attached to solid supports as opposed to proteins.[64] To date, the assay has been most useful in quantifying thiols grafted onto the surface of solid supports that are not disadvantaged by inaccessibility issues.[30]

With respect to surface area, the particles were generally nonporous further corroborating our hypothesis that thiol inaccessibility negatively influenced the Ellman's assay and the overall nitrosation efficiency (Table 2). A concomitant decrease in porosity was observed as the concentration of MPTMS in the particles increased from 40−75 mol %. Furthermore, incubating the 75 mol % MPTMS (balance TEOS, 718.0 ± 51.7 nm) particles with a reducing agent (dithiothreitol) before nitrosation did not significantly increase the NO storage capacity (2.73 μmol mg^{-1}) illustrating that the thiols accessible to nitrous acid do exist in the reduced form. Thus, the nitrosation efficiencies <100% are attributed to thiols buried deep within the nonporous particles that are solvent inaccessible. Of note, the degree of nitrosation efficiency did not correlate with porosity. The lower nitrosation efficiencies for the more porous particles (i.e., 25 and 40 mol % MPTMS) may be attributed to the greater error associated with measuring low levels of NO release and limited sulfur content.

The effect of copper on NO release was investigated as a function of copper concentration. These assays were performed using Cu(II) via $CuBr_2$ because of the insolubility of Cu(I) compounds in aqueous solutions.[65] As expected, the NO release from the RSNO-modified particles correlated with the copper concentration (Figure 7) with the greatest copper concentration examined (25 μM) generating the maximum NO release (∼45 ppb mg^{-1} s^{-1}).

The use of RSNO-modified particles for biomedical application likely necessitates an NO release trigger other than light or large concentrations of free copper ions.[66−68] We thus evaluated NO release from the particles via thermal degradation at 37 °C

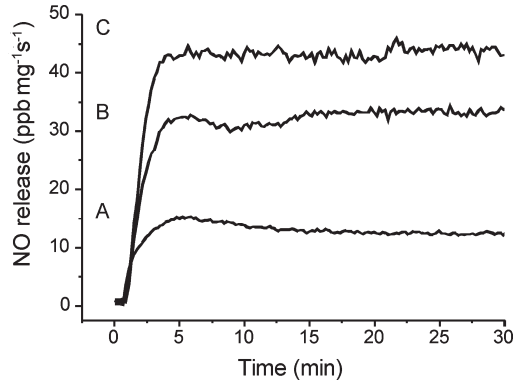

Figure 7. Representative nitric oxide release from RSNO-modified 75 mol % MPTMS (balance TEOS) particles in the presence of (A) 0, (B) 10, and (C) 25 μM $CuBr_2$/PBS solution at 0 °C. Note: 0 μM $CuBr_2$ is 500 μM DTPA (pH 7.4 PBS).

Table 3. Instantaneous NO Release Levels of S-Nitrosothiol-Modified Silica Particles at 37 °C in 500 μM DTPA (pH 7.4 PBS) and Shielded from Light

time (h)	instantaneous NO release (ppb mg^{-1} s^{-1})[a]
0	1205.7 ± 22.4
0.5	481.2 ± 7.7
1	355.7 ± 7.7
6	74.9 ± 0.7
12	33.2 ± 0.4
24	12.6 ± 0.2
48	2.50 ± 0.07

[a] Averages are calculated from n = 3 syntheses.

using 75 mol % MPTMS (balance TEOS, 718.0 ± 51.7 nm) as a model system. Particles were introduced into 500 μM DTPA (pH 7.4 PBS), maintained at 37 °C and shielded from external light while monitoring NO release over 48 h (Table 3). Under these conditions, the particles released a total of 1.17 μmol NO mg^{-1} with a corresponding half-life of 2.95 h. When compared to the total amounts released after 5 h using 200 W irradiation (3.15 μmol mg^{-1}, Table 2), the discrepancy may be attributed to inability to measure NO at low levels beyond 48 h and/or loss of NO through its reaction with oxygen present in the soak solutions.[61] As evident by a pink hue, the particles still contained a portion of their NO payload even after 48 h of thermally initiated release.

The total amount of NO loading on the RSNO-modified particles equals or exceeds most previously reported NO storage vehicles. For example, Stöber-synthesized *N*-diazeniumdiolate-modified silica particles[24] were reported to store approximately 1.7 μmol NO mg^{-1} while dendrimers[22] and surface-grafted silica particles[30] modified with RSNO moieties stored up to ~2 and ~0.138 μmol mg^{-1}, respectively. Although certain metal organic frameworks (MOFs) stored larger NO payloads (~7 μmol mg^{-1}),[69] the NO release from these vehicles is rapid and not controllable. In contrast, RSNO-modified particles enable extended NO release even under physiological conditions. Whereas pharmacological studies using the RSNO-modified silica particles are currently underway, the efficacy of NO release to inhibit platelet aggregation[22,70,71] and kill bacterial[72] using other vehicles (e.g., zeolites, MOFs, dendrimers, and silica particles) that release less NO has been established. On the basis of these previous reports, we find that the amounts and kinetics of NO release from the particles reported herein suggest encouraging pharmacological and biomedical potential.

4. CONCLUSIONS

The Stöber process enabled the facile synthesis of silica particles with tunable amounts of thiol functionality. Both the size and shape (spherical) of these organically modified particles were highly monodisperse. Furthermore, the size of the particles was readily tunable by varying the amount of water used in their synthesis. Nitrosating the thiols after particle formation resulted in the formation of macromolecular NO-donor scaffolds that store and release NO in proportion to the molar percentage of MPTMS used in their preparation. Under physiological conditions in the absence of light, the NO release durations from the particles exceeded 48 h. On the basis of these characteristics, we find that the particles hold great promise as NO-based therapeutics and/or dopants for NO-releasing polymeric coatings.[4−6]

AUTHOR INFORMATION

Corresponding Author
*E-mail: schoenfisch@unc.edu.

ACKNOWLEDGMENT

This research was supported by the National Institutes of Health (NIH EB000708). D.A.R. gratefully acknowledges a U.S. Department of Education Graduate Assistance in Areas of National Need (GAANN) Fellowship. The authors wish to thank Wesley L. Storm for assistance in acquiring the porosity data.

REFERENCES

(1) Fang, F. C. *J. Clin. Invest.* **1997**, *99*, 2818.
(2) Cooke, J. P. *Atherosclerosis Suppl.* **2003**, *4*, 53.
(3) Luo, J. D.; Chen, A. F. *Acta Pharmacol. Sin.* **2005**, *26*, 259.
(4) Frost, M. C.; Reynolds, M. M.; Meyerhoff, M. E. *Biomaterials* **2005**, *26*, 1685.
(5) Hetrick, E. M.; Schoenfisch, M. H. *Biomaterials* **2006**, *35*, 780.
(6) Varu, V. N.; Tsihlis, N. D.; Kibbe, M. R. *Vasc. Endovasc. Surg.* **2009**, *43*, 121.
(7) Seabra, A. B.; Duran, N. *J. Mater. Chem.* **2010**, *20*, 1624.
(8) Al-Sa'doni, H. H.; Ferro, A. *Curr. Med. Chem.* **2004**, *11*, 2679.
(9) Al-Sa'doni, H. H.; Ferro, A. *Mini-Rev. Med. Chem.* **2005**, *5*, 247.
(10) Butler, A. R.; Rhodes, P. *Anal. Biochem.* **1997**, *249*, 1.
(11) Hogg, N. *Free Radical Biol. Med.* **2000**, *28*, 1478.
(12) Williams, D. L. H. *Acc. Chem. Res.* **1999**, *32*, 869.
(13) Radomski, M. W.; Rees, D. D.; Dutra, A.; Moncada, S. *Br. J. Pharmacol.* **1992**, *107*, 745.
(14) Langford, E. J.; Brown, A. S.; Wainwright, R. J.; Debelder, A. J.; Thomas, M. R.; Smith, R. E. A.; Radomski, M. W.; Martin, J. F.; Moncada, S. *Lancet* **1994**, *344*, 1458.
(15) Laszlo, F.; Whittle, B. J. R.; Moncada, S. *Br. J. Pharmacol.* **1995**, *115*, 498.
(16) Ramsay, B.; Radomski, M.; Debelder, A.; Martin, J. F.; Lopez-jaramillo, P. *Br. J. Clin. Pharmacol.* **1995**, *40*, 101.
(17) de Souza, G. F. P.; Yokoyama-Yasunaka, J. K. U.; Seabra, A. B.; Miguel, D. C.; de Oliveira, M. G.; Uliana, S. R. B. *Nitric Oxide-Biol. Chem.* **2006**, *15*, 209.
(18) Garcia, J. A. D.; dos Santos, L.; Moura, A. L.; Ricardo, K. F. S.; Wanschel, A.; Shishido, S. M.; Spadari-Bratfisch, R. C.; de Souza, H. P.; Krieger, M. H. *J. Cardiovasc. Pharmacol.* **2008**, *51*, 78.

(19) Katayama, N.; Nakajou, K.; Komori, H.; Uchida, K.; Yokoe, J. I.; Yasui, N.; Yamamoto, H.; Kai, T.; Sato, M.; Nakagawa, T.; Takeya, M.; Maruyama, T.; Otagiri, M. *J. Pharmacol. Exp. Ther.* **2008**, *325*, 69.
(20) Katsumi, H.; Nishikawa, M.; Ma, S. F.; Yamashita, F.; Hashida, M. *J. Pharm. Sci.* **2004**, *93*, 2343.
(21) Katsumi, H.; Nishikawa, M.; Yamashita, F.; Hashida, M. *J. Pharmacol. Exp. Ther.* **2005**, *314*, 1117.
(22) Stasko, N. A.; Fischer, T. H.; Schoenfisch, M. H. *Biomacromolecules* **2008**, *9*, 834.
(23) Stasko, N. A.; Schoenfisch, M. H. *J. Am. Chem. Soc.* **2006**, *128*, 8265.
(24) Shin, J. H.; Metzger, S. K.; Schoenfisch, M. H. *J. Am. Chem. Soc.* **2007**, *129*, 4612.
(25) Shin, J. H.; Schoenfisch, M. H. *Chem. Mater.* **2008**, *20*, 239.
(26) Zhang, H. P.; Annich, G. M.; Miskulin, J.; Stankiewicz, K.; Osterholzer, K.; Merz, S. I.; Bartlett, R. H.; Meyerhoff, M. E. *J. Am. Chem. Soc.* **2003**, *125*, 5015.
(27) Polizzi, M. A.; Stasko, N. A.; Schoenfisch, M. H. *Langmuir* **2007**, *23*, 4938.
(28) Rothrock, A. R.; Donkers, R. L.; Schoenfisch, M. H. *J. Am. Chem. Soc.* **2005**, *127*, 9362.
(29) Brunner, T. J.; Wick, P.; Manser, P.; Spohn, P.; Grass, R. N.; Limbach, L. K.; Bruinink, A.; Stark, W. J. *Environ. Sci. Technol.* **2006**, *40*, 4374.
(30) Frost, M. C.; Meyerhoff, M. E. *J. Biomed. Mater. Res., Part A* **2005**, *72A*, 409.
(31) Brinker, J.; Scherer, G. *Sol-Gel Science*; Academic Press, Inc.: New York, 1990.
(32) Stöber, W.; Fink, A.; Bohn, E. *J. Colloid Interface Sci.* **1968**, *26*, 62.
(33) Gaslain, F. O. M.; Delacote, C.; Walcarius, A.; Lebeau, B. *J. Sol-Gel Sci. Technol.* **2009**, *49*, 112.
(34) Johnston, A. P. R.; Battersby, B. J.; Lawrie, G. A.; Trau, M. *Chem. Commun.* **2005**, 848.
(35) Johnston, A. P. R.; Battersby, B. J.; Lawrie, G. A.; Lambert, L. K.; Trau, M. *Chem. Mater.* **2006**, *18*, 6163.
(36) Lee, Y. G.; Park, J. H.; Oh, C.; Oh, S. G.; Kim, Y. C. *Langmuir* **2007**, *23*, 10875.
(37) Miller, C. R.; Vogel, R.; Surawski, P. P. T.; Jack, K. S.; Corrie, S. R.; Trau, M. *Langmuir* **2005**, *21*, 9733.
(38) Nakamura, M.; Ishimura, K. *J. Phys. Chem. C* **2007**, *111*, 18892.
(39) Nakamura, M.; Ishimura, K. *Langmuir* **2008**, *24*, 5099.
(40) Vogel, R.; Surawski, P. P. T.; Littleton, B. N.; Miller, C. R.; Lawrie, G. A.; Battersby, B. J.; Trau, M. *J. Colloid Interface Sci.* **2007**, *310*, 144.
(41) Walcarius, A.; Delacote, C. *Chem. Mater.* **2003**, *15*, 4181.
(42) Brown, J.; Richer, R.; Mercier, L. *Microporous Mesoporous Mater.* **2000**, *37*, 41.
(43) Richer, R.; Mercier, L. *Chem. Mater.* **2001**, *13*, 2999.
(44) De Canck, E.; Lapeire, L.; De Clercq, J.; Verpoort, F.; Van Der Voort, P. *Langmuir* **2010**, *26*, 10076.
(45) Osterholtz, F. D.; Pohl, E. R. *J. Adhes. Sci. Technol.* **1992**, *6*, 127.
(46) Tan, B.; Rankin, S. E. *J. Phys. Chem. B* **2006**, *110*, 22353.
(47) Albert, K. *J. Sep. Sci.* **2003**, *26*, 215.
(48) Bogush, G. H.; Tracy, M. A.; Zukoski, C. F. *J. Non-Cryst. Solids* **1988**, *104*, 95.
(49) Van Helden, A. K.; Jansen, J. W.; Vrij, A. *J. Colloid Interface Sci.* **1981**, *81*, 354.
(50) Huang, Y.; Pemberton, J. E. *Colloid Surf., A* **2010**, *360*, 175.
(51) Kim, J. W.; Kim, L. U.; Kim, C. K. *Biomacromolecules* **2007**, *8*, 215.
(52) Meng, Z.; Xue, C. Y.; Zhang, Q. H.; Yu, X. H.; Xi, K.; Jia, X. D. *Langmuir* **2009**, *25*, 7879.
(53) Park, S. K.; Do Kim, K.; Kim, H. T. *Colloid Surf., A* **2002**, *197*, 7.
(54) Yoo, J. W.; Yun, D. S.; Kim, H. J. *J. Nanosci. Nanotechnol.* **2006**, *6*, 3343.
(55) Kim, S. S.; Kim, H. S.; Kim, S. G.; Kim, W. S. *Ceram. Int.* **2004**, *30*, 171.
(56) Rahman, I. A.; Vejayakumaran, P.; Sipaut, C. S.; Ismail, J.; Abu Bakar, M.; Adnan, R.; Chee, C. K. *Colloid Surf., A* **2007**, *294*, 102.
(57) Branda, F.; Silvestri, B.; Luciani, G.; Costantini, A. *Colloid Surf., A* **2007**, *299*, 252.
(58) Wang, P. G.; Xian, M.; Tang, X. P.; Wu, X. J.; Wen, Z.; Cai, T. W.; Janczuk, A. J. *Chem. Rev.* **2002**, *102*, 1091.
(59) Bartberger, M. D.; Houk, K. N.; Powell, S. C.; Mannion, J. D.; Lo, K. Y.; Stamler, J. S.; Toone, E. J. *J. Am. Chem. Soc.* **2000**, *122*, 5889.
(60) Dicks, A. P.; Swift, H. R.; Williams, D. L. H.; Butler, A. R.; AlSadoni, H. H.; Cox, B. G. *J. Chem. Soc., Perkin Trans. 2* **1996**, 481.
(61) Grossi, L.; Montevecchi, P. C. *Chem.—Eur. J.* **2002**, *8*, 380.
(62) Shishido, S. M.; de Oliveira, M. G. *Photochem. Photobiol.* **2000**, *71*, 273.
(63) Matsuda, A.; Kobayashi, H.; Itoh, S.; Kataoka, K.; Tanaka, J. *Biomaterials* **2005**, *26*, 2273.
(64) Badyal, J. P.; Cameron, A. M.; Cameron, N. R.; Coe, D. M.; Cox, R.; Davis, B. G.; Oates, L. J.; Oye, G.; Steel, P. G. *Tetrahedron Lett.* **2001**, *42*, 8531.
(65) Crichton, R. R.; Pierre, J. L. *Biometals* **2001**, *14*, 99.
(66) O'Halloran, T. V.; Culotta, V. C. *J. Biol. Chem.* **2000**, *275*, 25057.
(67) Walshe, J. M. *Ann. Clin. Biochem.* **2003**, *40*, 115.
(68) Valko, M.; Morris, H.; Cronin, M. T. D. *Curr. Med. Chem.* **2005**, *12*, 1161.
(69) McKinlay, A. C.; Xiao, B.; Wragg, D. S.; Wheatley, P. S.; Megson, I. L.; Morris, R. E. *J. Am. Chem. Soc.* **2008**, *130*, 10440.
(70) Wheatley, P. S.; Butler, A. R.; Crane, M. S.; Fox, S.; Xiao, B.; Rossi, A. G.; Megson, I. L.; Morris, R. E. *J. Am. Chem. Soc.* **2006**, *128*, 502.
(71) Xiao, B.; Wheatley, P. S.; Zhao, X. B.; Fletcher, A. J.; Fox, S.; Rossi, A. G.; Megson, I. L.; Bordiga, S.; Regli, L.; Thomas, K. M.; Morris, R. E. *J. Am. Chem. Soc.* **2007**, *129*, 1203.
(72) Hetrick, E. M.; Shin, J. H.; Stasko, N. A.; Johnson, C. B.; Wespe, D. A.; Holmuhamedov, E.; Schoenfisch, M. H. *ACS Nano* **2008**, *2*, 235.